Published in: proceedings of the 9th European Conference on Industrial Furnaces and Boilers,
April 2011, Estoril, Portugal, CENERTEC (Ed.), Portugal

Development of an advanced CFD model for ash deposit and aerosol formation in biomass fired boilers

Kai Schulze [1], Robert Scharler [1,2,3] Ingwald Obernberger [1,2,3]

[1]Bioenergy 2020+ GmbH, Inffeldgasse 21b, A-8010 Graz, Austria;
[2]BIOS BIOENERGIESYSTEME GmbH, Inffeldgasse 21b, A-8010 Graz, Austria;
[3]Institute for Process and Particle Engineering, Graz University of Technology, Austria;
Email: kai.schulze@bioenergy2020.eu, scharler@bios-bioenergy.at, ingwald.obernberger@tu-graz.at

ABSTRACT

A CFD based deposit formation model for biomass fired boilers has been developed. The model considers the condensation of ash vapours, deposition of coarse salt-rich and silica-rich fly ash particles, brittle and ductile erosion of the deposit layer by non-sticky particles, aerosol formation and deposition under consideration of a single particle size class. Furthermore, the influence of the growing deposit layer on heat transfer (heat conduction, radiative emissivity of the surfaces) in the furnace and the boiler is taken into account.

The model has been evaluated concerning its applicability as process analysis and design tool for biomass combustion plants. For this purpose, test runs with a small-scale, fixed bed pellet furnace (70 kW_{th} nominal boiler capacity) and a medium-scale grate furnace with a 10 MW_{th} thermal oil boiler (fuels: fibre board, sawdust) were performed. The modelling results were validated against deposit formation and dust emission measurements (mass and chemical composition) performed at different locations of the plants.

The numerical results show the interaction between the involved chemical reactions within the turbulent reactive flow, condensation, fine particle formation as well as deposition of coarse fly ash particles. While the description of the ash vapours regarding condensation and fine particle formation already delivers quantitatively correct results, the accuracy of the stickiness model of coarse fly ash particles has to be improved.

Keywords: biomass combustion, ash deposition, CFD simulation

1. INTRODUCTION AND OBJECTIVES

Nowadays, Computational Fluid Dynamics (CFD) has been well established as an engineering tool to optimise biomass furnaces and boilers regarding flow and gas phase combustion.

Since agricultural residues, olive residues or waste wood constitute an attractive alternative to common biomass fuels boiler manufacturers and operators have to find strategies to take into account the risk of ash related problems like slagging in furnaces, fouling as well as corrosion in boilers in order to be competitive. 3D CFD simulations can be applied for the purpose of a spatially resolved simulation and analysis of deposit and aerosol formation in dependence of relevant influencing parameters.

Therefore, at BIOENERGY 2020+ a detailed CFD model for ash deposit formation in biomass fired boilers has been developed. It considers the condensation of ash vapours, the deposition of coarse salt-rich and silica-rich fly ash particles, brittle and ductile erosion of the deposit layer by non-sticky particles, aerosol formation and deposition under consideration of a single particle size class as well as the influence of the growing deposit layer on heat transfer (heat conduction and radiative emissivity of the surfaces) in the boiler.

In order to evaluate the reliability and accuracy of the model, test runs for a 70 kW pellet fixed bed furnace and a 10 MW biomass grate furnace with fibre board and sawdust as fuels have been performed. The simulations were compared with measurements of deposited mass and chemical composition of the deposits in different plant zones as well as with dust emission measurements.

2. MODEL SETUP

OVERVIEW

The deposit formation model has been implemented in the CFD Code FLUENT 12 using user defined functions (UDF). The calculation of solid biomass combustion on the grate and the release of flue gas components from the fuel bed is performed using an empirical packed bed combustion model based on experimental data [11] in order to provide the boundary conditions for the subsequent simulation of the turbulent reactive flow. The calculation of gas phase combustion is based on the Realizable k-ε model for turbulence, the Discrete Ordinate Model for radiation and the Eddy Dissipation model in combination with a global methane 3-step reaction mechanism including the flue gas components CH_4, CO, CO_2, H_2, H_2O and O_2 for gas phase combustion. A detailed description of the CFD combustion model for biomass grate furnaces can be found in [11].

The deposit build-up is simulated within a post-processing step based on the flow and gas phase combustion simulation. The empirical packed bed combustion model was extended in order to calculate the release of ash vapours and the entrainment of coarse fly ash particles from the grate to provide the boundary conditions for the CFD simulation of ash deposit and aerosol formation. Subsequently, CFD simulations of ash vapour condensation on the boiler walls, aerosol formation and deposition on the boiler walls are performed. Furthermore, the calculation of the deposition of coarse fly ash particles on boiler walls is based on two different stickiness approaches - a viscosity approach for silica-rich particles and a melting approach for salt-rich particles.

The condensation of the ash vapours as well as the deposition of coarse fly ash particles and fine particles contribute to the time-dependent build-up of the deposit layer. The growth of the deposit layer influences the heat transfer due to changes of the thermal resistance and emissivity of the layer as a function of its chemical composition, temperature, structure and thickness. Furthermore, erosion of deposits by coarse fly ash particles is considered.

In the following, a short description of the most relevant sub-models for ash deposit formation is given:

WALL CONDENSATION AND FINE PARTICLE FORMATION

During solid fuel combustion, ash forming vapours are released from the fuel bed into the gas phase. The mass flux and the composition of the ash components depend on the temperature in the fuel bed as well as the composition of the fuel. Due to the cooling of the flue gas or the contact with cooled walls, the vapour pressure of the components decreases. If the vapour pressure becomes lower than the saturation pressure of the ash vapour, the aggregate state changes to liquid or solid phases. Consequently, fine particles are formed in the gas phase, which form deposits on walls or are emitted. Furthermore, when the vapour pressure on the wall is lower than in the boundary layer, condensation occurs.

Ash forming vapours are involved in a complex reaction system. Here, with exception of the kinetically limited formation of sulphates, it is assumed that reactions between ash forming vapours are fast in comparison to local residence time of the flue gas. In this case, the chemical composition can be determined by thermodynamic equilibrium calculations. The accuracy of the predicted compositions depends on the quality of the thermodynamic data of the ash components, which are reliable for most alkali salts [6]. In case of the formation of sulphates, a kinetic approach was applied. According to Christensen [4] the formation of SO_3 from precursors (SO_2) is limited rather then the final formation of sulphates. In this model, the global reaction rate according to Christensen based on an Arrhenius approach, was implemented in combination with the Eddy Dissipation Model. Furthermore, in order to reduce the mathematical effort to model the transport of the ash vapours, the deposit formation model considers the transport of the elements (C, S, Cl, K, Na) instead of ash forming species as these elements are the most relevant ones regarding aerosol formation in wood pellet boilers [3]. To calculate condensation fluxes to the walls or fine particle formation, ash vapour pressures of species are determined by thermodynamic equilibrium calculations in combination with the In-Situ Adaptive Tabulation Algorithm (ISAT) [8] for the reduction of calculation times.

The condensation of ash vapours is modelled based on a mass transfer approach using the analogy of mass transfer to the convective heat transfer to determine the mass transfer coefficient β ([2]). Here, $\dot{N}_{cond}$ represents the condensation flux per area, α the heat transfer coefficient, c_p the heat capacity and ρ the density of the flue gas.

$$\dot{N}_{cond} = \frac{\alpha}{c_p \cdot \rho} Le^{m-1} \cdot (c_\infty - c_w) \tag{0.1}$$

The Lewis number Le as well as the exponent m were set to unity. While for c_∞ thermodynamic equilibrium calculations are carried out only under consideration of gaseous components, for the wall concentration c_w also liquid and solid phases at the surfaces have to be considered. In this work, the components KCl, $(KCl)_2$, K_2SO_4, K_2CO_3, NaCl, $(NaCl)_2$ and Na_2SO_4 are considered as ash forming vapours.

Similarly to condensation, the calculation procedure is implemented to calculate the super-saturation of ash components in the flue gas to describe the nucleation of the ash vapour components as initial aerosol formation process. The nucleation rate is calculated according to Friedlander [5], which is based on the classical theory of nucleation:

$$I_{nucl} = 2 \cdot \frac{p_i}{\sqrt{2 \cdot \pi \cdot m_m \cdot k_B \cdot T}} \cdot V_m^{2/3} \cdot n_m \cdot \sqrt{\frac{\sigma \cdot V_m^{2/3}}{k_B \cdot T}} \cdot exp\left(-\frac{16 \cdot \pi \cdot \sigma^3 \cdot V_m^2}{3 \cdot (k_B \cdot T)^3 \cdot ln(S)^2} \right) \tag{0.2}$$

Here, p_i is the vapour pressure of the nucleating compound i, m_m is the mass of a molecule calculated from the molar weight and Avogadro's number, k_B the Stefan–Boltzmann constant, V_m is the volume of a molecule calculated from the liquid density and Avogadro's number, n_m is the molecule concentration in the gas, σ is the surface tension of the nucleating compound, S is the saturation ratio ($=p_i/p_{sat}$ with p_{sat} = saturation pressure of the nucleating compound).

Besides the formation of new particles by nucleation, the model also considers condensation of ash vapours on the surface of existing aerosol particles. For this purpose, the condensation flux is determined by

$$I_{cond} = \frac{F_i \cdot MW_i \cdot 6}{\rho_i \cdot d_p^3 \cdot \pi}$$

$$F_i = \frac{2 \cdot \pi \cdot D_i \cdot d_p \cdot (p_i - p_{i,sat}^*)}{k_B \cdot T} \tag{0.3}$$

with ρ_i as density of the condensing compound, D_i as diffusion coefficient of the condensing compound in the gas phase and MW_i as molecular weight of the condensing compound.

At the present state of development, a constant particle size (10^{-7} m) was assumed. Consequently, nucleation and condensation results in a change of the number of fine particles formed. The deposition of fine particles is considered by Fick´s law for diffusion and thermophoresis is according to:

$$v_{th} = \frac{\nu_{gas} \cdot K_{th}}{T_p} \nabla T_{gas} \tag{0.4}$$

K_{th} is the so-called thermophoretic coefficient, which is determined by Talbot [12], ν_{gas} the viscosity of the gas, T_p the temperature of the particle and ∇T_{gas} the local temperature gradient prevailing in the gas phase. Deposition mechanisms of fine particles due to inertial impaction, gravitational settling as well as diffusiophoresis are neglected up to now, but it is known, that they only play a minor role [3].

DEPOSITION OF COARSE FLY ASH PARTICLES

The transport of coarse fly ash is modelled using an Lagrangian approach, which is already implemented in the CFD code FLUENT (Discrete Phase Model). Once a particle impacts the wall, either its kinetic energy is high enough to rebound from the surface, or the particle sticks to the wall. The total sticking probability p_{tot} of the particle depends on the properties (sticking probabilities p) of the wall and the particle (Walsh [14])

$$p_{tot} = p_{wall} \cdot p_{part} + p_{wall} \cdot (1 - p_{part}) + (1 - p_{wall}) \cdot p_{part} \,. \tag{0.5}$$

In this model, a viscosity approach for silica-rich particles and a melting approach for salt-rich particles is used. The sticking probability of silica-rich particles is calculated by the ratio of the reference viscosity μ_{ref} and the viscosity of the particle at a certain temperature μ_{part}. While the viscosity of the silica-rich material is determined using a viscosity model of Urbain [13], the reference viscosity μ_{ref} is calculated as a function of the kinetic energy of the particle ([9]):

$$\log_{10}\left(\mu_{ref}\right) = -0.9699 \cdot \log_{10}\left(\frac{E_{kin}}{E_{kin,0}}\right) + 5.5962 \tag{0.6}$$

Here, the kinetic energies of the particles E_{kin} are normalized with the kinetic energy of the smallest particle ($E_{kin,0}$ = 4.35e^{-11} J) studied in the work of Srinivasachar et al. [10].

The melt approach according to Backman [1] was applied for salt-rich particles and deposit layers. Based on comparisons of experimental data from biomass fired boilers with thermodynamic calculations, the author derived a criteria of 15% molten phase of the ash, below which the particles are not sticky (sticking probability $p_{part,\ salts}$ = 0). Above this melt fraction, a linear correlation of the stickiness from 0 to 100% is assumed up to a melt fraction of 0.7 (flow condition for the ash [1]). Within the CFD code, the amount of the melt fraction is calculated by thermodynamic equilibrium calculations considering condensed phases (salt mixtures, slags).

Since a particle and a deposit layer consist of a mixture of salt and silica-rich material, the melt approach as well as the viscosity approach were combined using the mass weighted average of the stickiness probability of both models.

If the coarse fly ash particles do not stick on the walls, they rebound. Depending on the particle velocity and the impact angle, this process causes erosion of the deposit layer. In order to consider these erosion effects by coarse fly ash particles, the model from Neilson and Gilchrist which considers the two known main mechanisms, brittle erosion and ductile erosion was implemented.

3. TEST RUNS

PLANT DESCRIPTION AND OPERATING CONDITIONS

In order to evaluate the deposit formation model described in chapter 2, test runs with two different plants, a 70 kW wood pellet fixed bed furnace and a 10 MW_{th} biomass grate furnace including fuel analyses as well measurements of boiler heat load, air mass fluxes, conventional flue gas and dust measurements have been performed **(Fig.1)**. In addition, in the case of the small-scale furnace the mass and chemical composition of grate ash, fly ash and hard ash in different plant zones have been measured and in the case of the medium-scale combustion plant deposit probe measurements have been carried out.

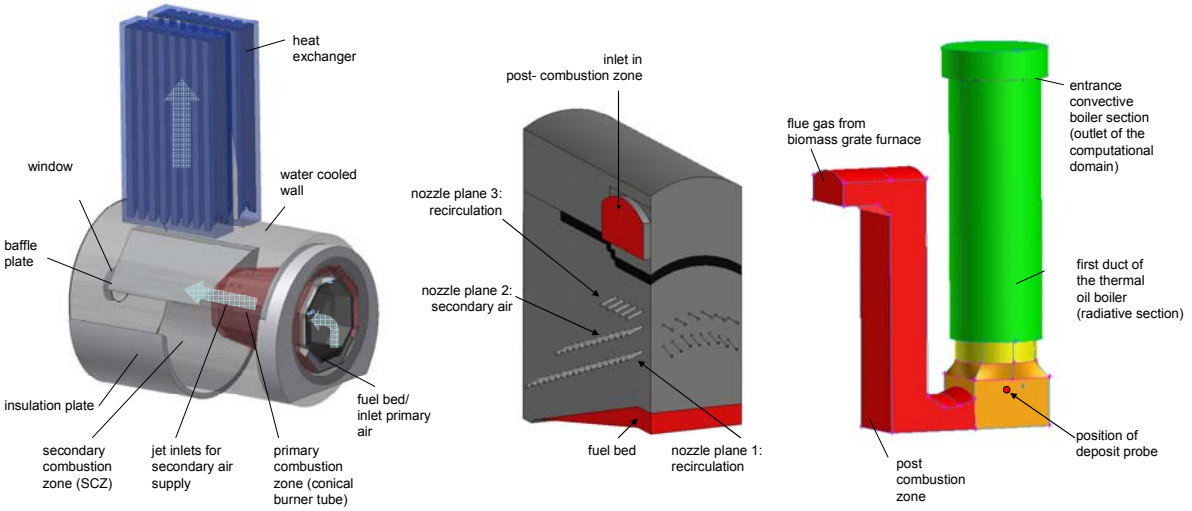

Fig. 1: Scheme of: left) the small-scale plant (70 kW boiler), middle) the 10 MW biomass grate furnace until the entrance in the post-combustion zone; right) the simulated section in the surrounding area of the deposit probe

Since the deposit formation simulations are very time-consuming, they have only be considered in the surrounding area of the deposit probe in the case of the medium-scale combustion plant. Within the frame of a previous simulation run, the kinetic conversion of sulphate precursors as well as the wall condensation fluxes in the biomass furnace were determined to gain the boundary conditions for the subsequent deposit formation simulation. While

Fig. 1 **(middle)** provides an overview about the biomass grate furnace,

Fig. 1 **(right)** illustrates the sections of the plant considered for the deposit formation simulations. The computational domain comprises the post combustion chamber of the furnace until the end of the radiation part of the thermal oil boiler. The deposit-probe measurements were carried in the entrance to the first duct of the thermal oil boiler (radiation part).

The most relevant operating conditions during the test runs as well as the chemical composition of the ash forming elements of the fuels are shown in **Table 1**. The small-scale plant

Fig. 1 **(left)** is divided into a primary combustion zone (PCZ) located in the rear part of the burner tube, which is cooled by the secondary air and a water cooled secondary combustion zone (SCZ). After the combustion of the fuel in the burner tube (PCZ), the released flue gas is mixed with secondary air supplied by nozzles at the exit of the burner tube. At the top of the SCZ, the heat exchanger tube bundle is installed. The automatic cleaning system for the heat exchanger tubes was not installed for the purpose of the model check.

Table 1: Operating conditions (left) and concentration of ash forming elements [mg/kg d.b.] in the fuels (right)

parameter	units	small-scale plant	medium-scale plant	
fuel		wood pellets	sawdust	fibre board
net calorific value	MJ/kg w.b	17,00	12,45	16,92
fuel flow rate	kg/h	16	3.469	2.647
C/H ratio	-	8,79	8,32	7,88
ash content	wt.% d.b.	0,40	0,31	1,49
moisture content	wt.% d.b.	6,8	30,8	6,3
boiler load	kW	74	13.200	12.400
primary air mass flux	kg/h	31	6.903	7.630
secondary air mass flux	kg/h	122	18.502	19.620
recirculation ratio	-	0,00	0,34	0,40
total air ratio	-	1,79	1,84	1,80
primariy air ratio	-	0,36	0,50	0,50
adiabatic flue gas temperature	°C	1.329	898	861
temperature cooling medium	°C	62	300	300

element	wood pellets	fibre board	sawdust
Si	199	225	787
Ca	1.000	898	2.080
Mg	118	117	266
K	402	318	639
Na	38,2	13,3	239
S	64,7	56,3	477
Cl	44	19,2	190
Zn	9,88	8,51	35,1
Pb	5	0	0
Fe	26,3	7,44	150
Mn	168	83,8	81,6
Al	34,2	11	846
P	49,5	19,2	0
Cu	0	0,697	2,05
Ti	1,89	0	0

TEST RUN RESULTS

Table 2 (left) shows the total mass of hard deposits, fine particle emissions and coarse fly ash emissions of the small-scale furnace over an operation time of 69 h at full load. The overall mass balance regarding ashes found in comparison to the ash input with the fuel closes well which underlines the plausibility of the measurements performed.

Table 2: Mass of ash deposits and emissions of the small- (left) and the medium scale furnace (right)

measurements in the small scale plant over an operation time of 69h

position	mass [g]
bottom ash inside the burner tube	420
bottom ash on the insulation plate	1698
deposits on burner tube walls	52
deposits on the baffle plate	131
deposits on cooled boiler walls of the SCZ	10
ash on window	33
ash on the surface of the heat exchanger	268
ash in the exhaust gas receiver	207
coarse fly ash emissions	194
fine particle emissions	110
sum of ash samples	3124
ash input according to fuel analysis	3165
rate of recovery [%]	99

flue gas measurements of boiler outlet (emission to atmosphere)

CO [ppm]	26
excess oxygen in flue gas [Vol.-%, dry base]	9,3
flue gas temperature of boiler exit [°C]	266
total dust [mg/Nm³] (13 Vol.-%O_2, dry flue gas)	21,2
PM1 [mg/Nm³] (13 Vol.-%O_2, dry flue gas)	7,65

measurements in the medium-scale plant over a period of 9 h

	mass fluxes [kg/h]	
position	fibre board	sawdust
bottom ash on the grate	1,43	16,75
coarse fly ash emissions	3,39	17,58
fine particle emissions	1,62	2,64
ash input according to fuel analysis	6,44	36,97

flue gas measurements of economiser outlet (before ESP)

CO [ppm]	8,9	10,1
excess oxygen in flue gas [Vol.-%, dry base]	9,5	9,7
flue gas temperature of boiler exit [°C]	185,5	184,3
total dust [mg/Nm³] (13 Vol.-%O_2, dry flue gas)*	347	115,8
PM1 [mg/Nm³] (13 Vol.-%O2, dry flue gas)j*	52,13	37,5

* measurment at the outlet of the economiser of the plant

Furthermore, the measurements of the medium-scale plant are shown. Based on total dust and fine particle measurements, the amount of bottom ash was determined from the ash input according to the fuel analysis.

In all cases, the burnout conditions were very good as indicated by the low CO emissions.

The release of the ash vapours and the entrainment of coarse fly ash particles from the fuel bed depend on the chemical composition of the fuel and the local conditions in the fuel bed (local temperature, stoichiometry and flue gas velocity in the bed). If experimental data regarding mass and elemental balances of the biomass combustion plants are available in a good quality, the release of ash vapours and fly ash particles can be determined from test runs. Since this precondition for the mass balance data was fulfilled for the small-scale combustion plant, the released mass of the aerosol forming elements K, Na, Cl and S from the fuel bed was calculated from the difference of the mass of these elements found in the bottom ash fractions and in the coarse fly ash fractions (under the assumption that the coarse fly ash has the same composition than the bottom ash when entrained from the fuel bed) and the amount of these elements supplied with the fuel. The amount of coarse fly ash entrained from the fuel bed was calculated by subtracting the amount of bottom ash formed and the amount of ash vapours released from the total mass of ash supplied with the fuel. Since the deposits from the exhaust gas channel mainly consist of coarse fly ash particles, their chemical composition was used to calculate the particle stickiness properties of the model.

In the case of the medium-scale combustion plant, the release of the ash vapours had to be estimated from previous lab-scale investigations using similar biomass fuels and operational conditions [7], since the elemental ash balance could not be closed. Table 3 right gives an overview about the percentage of aerosol forming elements which are released from the fuel to the gas phase. Additionally, the chemical composition of the coarse fly ash particles entrained from the fuel bed is shown, which is used to calculate the coarse fly ash stickiness of the model. In the case of the small-scale furnace the chemical composition of coarse fly ash particles found in deposits from the exhaust gas channel has been taken, in the case of the medium-scale plant the coarse fly ash particles found in the cyclone after the economiser were used.

Table 3: Percentage of aerosol forming elements (wt.%) released from the fuel (right) and chemical composition of the coarse fly ash particles (wt.% d.b.) entrained from the fuel bed (left)

	small-scale plant	medium scale plant	
element	wood pellets	fibre board	sawdust
Si	3.35%	4.92%	4.74%
Ca	25.20%	21.60%	23.80%
Mg	3.39%	2.71%	2.87%
K	12.30%	4.13%	4.43%
Na	0.65%	0.61%	0.48%
S	0.34%	1.35%	1.41%
Cl	0.07%	0.45%	0.48%
Zn	0.04%	0.14%	0.14%
Pb	0.00%	0.02%	0.02%
Fe	0.65%	1.18%	1.31%
Mn	4.78%	1.75%	2.00%
Al	0.54%	4.03%	3.40%
P	1.26%	0.93%	0.94%
Ti	0.04%	0.00%	0.00%

element	small-scale plant	medium scale plant	
	wood pellets	fibre board	sawdust
K	25	37	45
Na	58	75	35
S	87	85	85
Cl	96	100	100

4. SIMULATION RESULTS

In order to illustrate the chemical interactions of the ash forming vapours in the plants, some fundamental simulation results regarding the flue gas temperature and the kinetically limited conversion of sulphate precursors (H_2S, S, SO_2) to SO_3 and sulphates is shown. Afterwards, selected results regarding condensation, fine particle formation as well as the deposition behaviour of coarse fly ash particles are given. Finally, in the case of the small-scale plant, simulations have been performed considering all sub-models implemented in the deposit formation model. Ash deposit rates as well as the emissions of coarse fly ash and fine particles are compared with measurements to check and evaluate the simulations.

FLUE GAS TEMPERATURE AND SULPHUR KINETICS

Fig. 2 shows the molar ratio of gaseous sulphates and SO_3 in the flue gas in a vertical cross section of the plant, which is formed by the oxidation of sulphate precursors (S, H_2S, SO_2). Despite of the high gas temperatures inside the burner tube (see **Fig. 2 a**) the lack of oxygen in the PCZ inhibits the oxidation of the released volatile sulphur species. Subsequently, after mixing with secondary air this

restriction is removed and the concentration of sulphates and SO_3 increases. Subsequently, due to the formation of fine particles and condensation of the ash vapours on the walls, the molar fraction decreases.

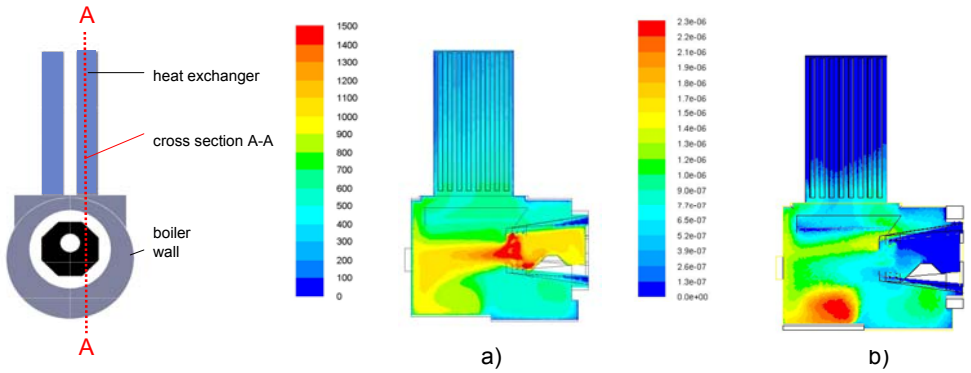

Fig. 2: a) Calculated flue gas temperatures (°C) in the vertical cross section A-A of the boiler; b) molar fraction [mol/mol] of gaseous sulphates and SO_3 formed by the oxidation of sulphur precursors

In **Fig. 3** the conversion rates of the released sulphate precursors to sulphates and SO_3 are shown for all test cases. Here, the molar ratio is defined as the sum of sulphur located in fine particles and deposits to the amount of sulphur in the released sulphur precursors. It can be seen, that the sulphur conversion varies between 40 % and 87 %.

plant	fuel	sulphur conversion [mol/mol]
small-scale furnace	wood pellet	0.66
medium-scale furnace	sawdust	0.87
medium-scale furnace	fibre board	0.40

Fig. 3: Conversion rates of sulphur precursors to gaseous sulphates and SO_3

FINE PARTICLE FORMATION AND CONDENSATION

Due to the oxidation of SO_2 gaseous sulphates are formed in the SCZ (**Fig. 4, left**).

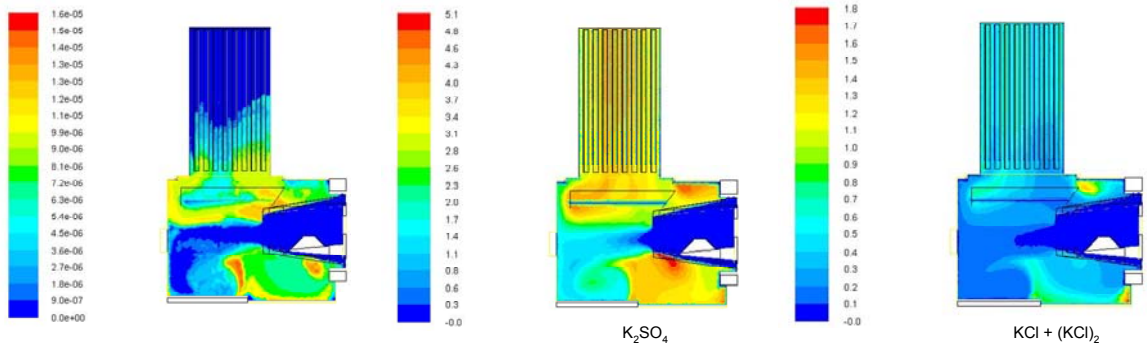

Fig. 4: Simulation results regarding left) the concentration field of gaseous K_2SO4 [kmol/m³] middle) the fine particles formed by nucleation/condensation of gaseous K_2SO_4 [mg/Nm³ dry flue gas, 13 % O_2], left) the fine particles formed by nucleation/condensation of KCl and $(KCl)_2$ [mg/Nm³ dry flue gas, 13 % O_2]

Simultaneously, if the temperature is below 900°C, the amount of gaseous K_2SO_4 is decreased by the formation of fine particles. Hence, the maximum sulphate concentrations can be found in a boundary zone between the formation zone of sulphates and regions of fine particle formation. In **Fig. 4 (middle)**, the concentration field of the fine particles formed by nucleation and condensation of K_2SO_4 as well as the concentration field of fine particles formed by KCl and the dimer $(KCl)_2$ **(right)** are shown. The different fine particle formation behaviour which can be observed in the burner tube and in the SCZ is based on the different flue gas temperatures in these regions. Since the temperatures inside the burner (see **Fig. 2 a**) are above 1,000°C, the initial formation of fine particles can only occur at the outlet of the burner. In the cooled SCZ, sulphates are formed in the hot zone near the outlet of the PCZ. Fine particles consisting of chlorides are formed in the boundary zones near the cooled wall.

In **Fig. 5** the total concentration field of the fine particles is illustrated. Furthermore, the chemical compositions of the fine particles are compared with fine particle measurements. It is found that the amount of sulphate in the fine particles is slightly overpredicted by the model. The averaged concentration of the sum of all fine particles at the furnace outlet (9.92 mg/Nm³ dry flue gas, 13 % O_2) is in good agreement with experimental data (7.65 mg/Nm³ dry flue gas, 13 % O_2).

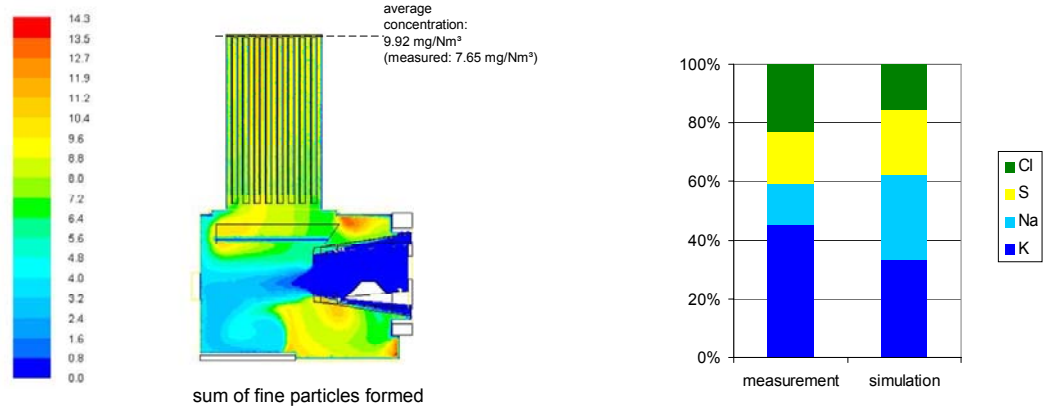

Fig. 5: Simulation results regarding aerosol formation: left) total fine particle emissions [mg/Nm³ dry flue gas, 13 % O_2]; right) comparison of measurement and simulation results regarding the chemical composition of fine particles [mol-% d.b.]

Fig. 6 (left) illustrates the wall temperatures of the simulated sections of the medium-scale plant (furnace section and radiative boiler section), the overall deposit mass flux caused by condensation and fine particle precipitation (middle) as well as the mass flux by KCl precipitation of fine particles and condensation on the walls (right).

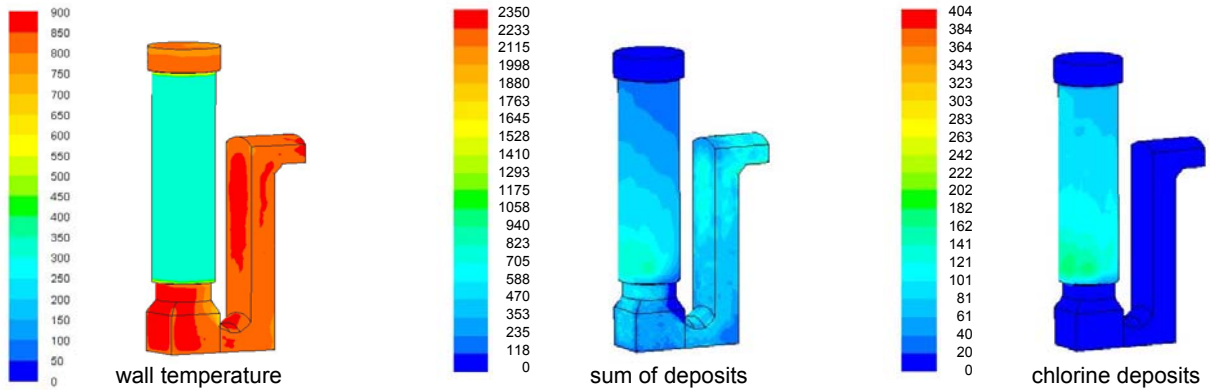

Fig. 6: left) wall temperature [°C] of the simulated section of the medium-scale combustion plant; middle) overall deposit mass flux caused by condensation and fine particle precipitation [mg/m²h]; right) deposit mass flux of chlorine [mg/m²h] caused by condensation and fine particle precipitation; fuel: saw dust

A different deposit formation behaviour can be observed at the cooled walls the thermal oil boiler and the insulated walls of the post-combustion chamber. Due to the different wall temperatures and the different vapour pressures of the chlorines and sulphates at the surfaces of the walls the deposition of chlorides occurs only at temperatures below 600°C. In contrast, sulphate containing fine particles are formed already at temperatures below 900°C. Within this boiler section, the primary deposit formation mechanism caused by ash forming vapours is condensation, thermophoresis and diffusion of fine particles play only a minor role.

In **Fig. 7** a comparison of experimental and numerical data regarding the chemical composition of the deposit probe concerning the considered elements K, Cl, Na and S is shown. The deposits were formed by precipitation of fine particles as well as by condensation of ash forming vapours on the cooled wall. While for sawdust, a good agreement can be found, for the fuel fibre board, the amount of sulphates calculated is somewhat to low.

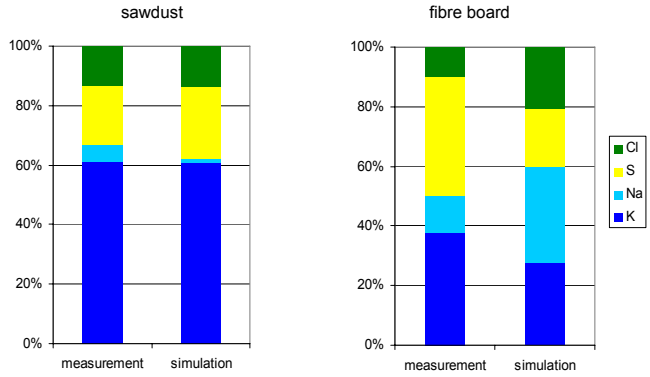

Fig. 7: Comparison of experimental and numerical results regarding the chemical composition [mol -%] of the deposit layer formed; left: sawdust, right: fibre board

DEPOSITION OF COARSE FLY ASH PARTICLES

Fig. 8 a shows calculated deposition mass fluxes caused by the impaction of coarse fly ash particles in the small-scale plant (other deposition processes are not considered). The main part of the particles is captured by the inner hot walls of the burner tube. Also in the SCZ the model predicts a high sticking probability of the particles impacting on the insulation plate. Only 3 wt.% of the released particles reach the outlet of the heat exchanger (measured value approximately 50 %). As a consequence, the influence of the erosion model can be neglected within this simulation because the high stickiness results in no relevant particle rebound rates after their impact on the walls.

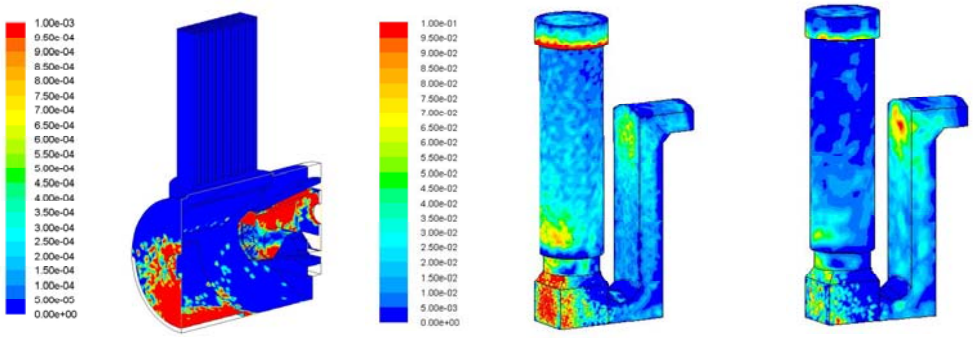

Fig. 8: Deposit mass flux of coarse fly ash particles (kg/m²h); a) small-scale plant (wood pellets), b) medium-scale plant (fibre board); c) medium-scale plant (sawdust)

Since the mass fraction of silica-rich components of the particles amounts to 98 %, the stickiness of the particles is almost entirely calculated by the viscosity approach. Consequently, the model predictions regarding the reference viscosity should be improved. For this purpose, experimental investigations concerning the reference viscosity of the stickiness approach regarding silica-rich particles (e.g. described in [9]) are necessary to improve the stickiness approach used.

Fig 8 b) and **c)** show the deposit build-up caused by the impaction of coarse fly ash particles in the simulated sections of the medium-scale plant. Also in this case, the stickiness of the coarse fly ash particles is over-predicted, since most of the particles are captured on the walls of the post-combustion channel. As a consequence, measured coarse fly ash emissions after the economiser (sawdust: 78 mg/Nm³ dry flue gas, 13 % O_2; fibre board: 294 mg/Nm³ dry flue gas, 13 % O_2) are significant higher than the numerical results at the end of the computational domain (sawdust: 33 mg/Nm³ dry flue gas, 13 % O_2; fibre board: 176 mg/Nm³ dry flue gas, 13 % O_2).

OVERALL DEPOSIT BUILD-UP

In **Fig. 9** the experimental data from test runs of the small-scale furnace are compared with a simulation considering condensation of ash vapours, aerosol formation and deposition as well as deposition of coarse fly ash particles (overall model).

	measured deposit mass [g]	simulation result (overall model) [g]
deposition flux	535	910
emission of fine particles (PM1)	110	98
emission of coarse fly ash particles	194	25

Fig. 9: Comparison of experimental and numerical data (from the overall model) regarding deposition and emission results

The comparison shows that the measured deposition flux is lower than the simulation result almost by a factor of two, while the predicted fine particle emissions are in good agreement with the measurements. As already discussed in the previous section, the reasons can mainly be found in the overestimation of the stickiness of the coarse fly ash particles. In addition, effects that have not been taken into account by the model contribute to deviations to the numerical results, e.g. particle re-entrainment by shear forces of the flue gas or shedding of the deposit layers.

Since the accuracy of the model regarding the stickiness of the coarse fly ash particles in not sufficient to describe the chemical composition and thickness of deposit layers, its influence on heat transfer in the furnace and the boiler is not discussed in this paper. During the test run of the small-scale furnace, an increase of the flue gas temperature of 26 K was measured over a period of 40 h. It follows that the heat flux to the boiler is reduced by 1 kW after this time (1.4 % of the boiler output, 25 W/h).

5. SUMMARY AND CONCLUSIONS

The numerical results gained by the application of the deposit formation model for two different plant sizes of fixed bed biomass boilers and three different fuels illustrate the contribution of different mechanisms to deposit build-up and aerosol formation. The influence of chemical reactions, aerosol formation, condensation as well as the deposition of coarse fly ash particles is shown.

Comparisons of model predictions with experimental findings regarding the emissions of coarse fly ash particles show, that the stickiness of the silica-rich particles is over-predicted by the model. The assumption of a material independent reference-viscosity, which was developed for coal ashes, seems not to be applicable for biomass ashes. In order to increase the accuracy of the stickiness model for silica rich particles, the experimental determination of the reference viscosity as a function of the kinetic energy of the particles for different biomass fuels is necessary.

The predictions of the aerosol formation model in combination with the condensation model regarding fine particle concentrations and chemical compositions are in good agreement with experiments. The chemical composition of the deposit probe measurements of the medium-scale plant are also in good agreement with simulations in case of sawdust. In the case of the fibre board residues, the sulphate concentration is under-predicted, which may be due to the sulphur kinetics used. Nevertheless, some deviations from the measurement results must be expected, since the model contains some simplifications (e.g. constant material properties) as well as no modelling of the particle size distribution. Furthermore, temperature fluctuations in the flue gas prevailing during the test runs have an impact on the ash chemistry (e.g. sulphation rates).

Concluding, it can be stated that an advanced tool for an efficient design of biomass furnaces and boilers is under development. The influence of the fuel fired and operation conditions on deposit and aerosol formation processes can be investigated in detail considering the relevant mechanisms already in the design phase of the plant and thus allowing for appropriate measures in order to reduce ash deposit formation and to take proper choices regarding material selection in terms of corrosion issues. The model can already deliver quantitatively correct results regarding fine particle formation and condensation. In order to achieve better predictions regarding the overall deposit build-up, a better description of the stickiness behaviour of coarse fly ash particles should be implemented. As further model development steps, the consideration of aerosol particle size distributions as well as the deposit build-up in heat exchanger tube bundles are foreseen. Moreover, experiments in a specially designed biomass-fired drop-tube furnace with an implemented deposit probe are planned to achieve reliable data regarding erosion and stickiness.

6. ACKNOWLEDGEMENTS

The work presented was supported by the Kplus program of the BIOENERGY 2020+. The financial support of the Austrian Research Promotion Agency as well as of the state governments of Lower Austria and Styria and of the City of Graz as well as of the companies BIOS BIOENERGIESYSTEME GmbH, MAXXTEC AG, Hovalwerk AG, KWB Kraft und Wärme aus Biomasse GesmbH is gratefully acknowledged. The deposit measurements were performed in cooperation with Hovalwerk AG, Liechtenstein, BIOS BIOENERGIESYSTEME GmbH, Austria and MAXXTEC AG, Germany.

7. REFERENCES

[1] R. Backman, M. Hupa, B-J. Skrifvars, Predicting superheater deposit formation in boilers burning biomass, Proceedings of the conference on impact of mineral impurities in solid fuel combustion (1999) 405-416.

[2] H. D. Baehr, K. Stephan, Wärme- und Stoffübertragung, 2nd Edition, Springer, Berlin. 1996

[3] T. Brunner, G. Bärnthaler, I. Obernberber, Evaluation of parameters determining PM emissions and their chemical composition in modern residential biomass heating appliances. In: Proc. of the int. Conf. World BIOENERGY 2008, (2008), Jönköping, Sweden, ISBN 978-91-977624-0-3, pp.81-86, Swedish Bioenergy Association (Ed.), Stockhm, Sweden

[4] K. A. Christensen, M. Stenholm, H. Livberg : The formation of submicron aerosol particles, HCl and SO2 in straw fired boilers, Journal of Aerosol Science (1998), 29, 421–444

[5] S. K. Friedlander, Smoke, dust and haze; John Wiley & Sons, New York (1977) ISBN 0-471-01468-0.

[6] D. Lindberg, R. Backman, P. Chartrand et. al. : Towards a comprehensive thermodynamic database for ash-forming elements in biomass and waste combustion - current situation and future developments, . In: Proc of the Int. Conf. “Impacts of Fuel Quality on Power Production”, (2010), Lapland, Finland

[7] S.C. van Lith, P.A. Jensen, F.J. Frandsen, P. Glarborg: Release of inorganic elements during wood-firing on a grate, . In: Proc of the Int. Conf. “Impacts of Fuel Quality on Power Production”, EPRI report No. 1014551 (2007), pp.7-95 to 7-113, EPRI (Ed.), Palo Alto, CA; USA

[8] S. B. Pope, ISAT-CK (Version 3.0) User’s Guide and Reference Manual, Ithaca Combustion Enterprise, LLC, Ithaca, USA (2000)

[9] K. Schulze, G. Hofmeister, M. Joeller et al., Development and evaluation of a flexible model for CFD simulation of ash deposit formation in biomass fired boilers. In: Proc of the Int. Conf. “Impacts of Fuel Quality on Power Production”, EPRI report No. 1014551 (2007), pp.7-95 to 7-113, EPRI (Ed.), Palo Alto, CA; USA

[10] S. Srinivasachar, J. J. Helble, A. A. Boni: An Experimental Study of the Inertial Deposition of Ash under Coal Combustion Conditions, 23rd Symposium on Combustion, (1990) The Combustion Institute, 1305-1312.

[11] R. Scharler, Entwicklung und Optimierung von Biomasse-Rostfeuerungen durch CFD-Analyse, Ph.D. thesis, Graz University of Technology, Graz, Austria (2001)

[12] L. Talbot, R. K. Cheng, R. W. Schefer et al., Thermophoresis of particles in a heated boundary layer, Journal of Fluid Mechanics, 101 (1980) 737-758.

[13] G. Urbain, F. Cambier, M. Deletter, Viscosity of silicate melts, Transactions and Journal of the British Ceramic Society (1981) 80, 139-141

[14] P. M. Walsh, A. N. Sayre, D. O. Loehden et al., Deposition of bituminous coal ash on an isolated heat exchanger tube: effects of coal properties on deposit growth, Progress in Energy Combustion Science 16 (1990) 327-346.